



**ISLAMIC UNIVERSITY OF TECHNOLOGY**  
**ORGANIZATION OF ISLAMIC COOPERATION**



# **VIBRATION ANALYSIS OF DIFFERENT AIRFOILS OF AIRCRAFT WING**

**B.Sc. Engineering (Mechanical) Thesis**

**AUTHORED BY:**

**ZAHIN MOSTAKIM**

Student ID: 151414

**KAISAR AHAMMED SAJIB**

Student ID: 151415

**MOAZ EBON ZABAL**

Student ID: 151417

**SUPERVISED BY:**

**PROF. DR. MD. ZAHID HOSSAIN**

Head, Department of Mechanical and Production Engineering

Islamic University of Technology (IUT)

**Department of Mechanical and Production Engineering (MPE)**

**Islamic University of Technology (IUT)**

**NOVEMBER 2019**

## **CERTIFICATE OF RESEARCH**

The thesis titled **“VIBRATION ANALYSIS OF DIFFERENT AIRFOILS OF AIRCRAFT WING”** submitted by **ZAHIN MOSTAKIM (151414), KAISAR AHAMMED SAJIB (151415), MOAZ EBON ZABAL (151417)** has been accepted as satisfactory in partial fulfillment of the requirement for the Degree of Bachelor of Science in Mechanical & Chemical Engineering on November, 2019.

Supervisor

---

**PROF. DR. MD. ZAHID HOSSAIN**

Head, Department of Mechanical & Production  
Engineering (MPE)

Islamic University of Technology (IUT)

## **DECLARATION**

---

This is hereby declared that the work presented in this thesis is an outcome of the analysis, simulation & research carried out by the author themselves under the watchful supervision of Prof. Dr. Md. Zahid Hossain and their thesis and any part of the report has not been submitted elsewhere for the award of any degree or diploma.

### **Signature of the Authors**

---

**ZAHIN MOSTAKIM**

Student ID: 151414

---

**KAISAR AHAMMED SAJIB**

Student ID: 151415

---

**MOAZ EBON ZABAL**

Student ID: 151417

### **Signature of the Supervisor**

---

**PROF. DR. MD. ZAHID HOSSAIN**

Head, Department of Mechanical & Production  
Engineering (MPE)

Islamic University of Technology (IUT)

## **ACKNOWLEDGEMENTS**

We would like to express our deepest appreciation to our respectable supervisor **PROF. DR. MD. ZAHID HOSSAIN and NAGIB MEHFUZ sir** for his support, guidance, care, tutelage, motivation and patience throughout the research period. We appreciate his talent and the encouragement which he provided us throughout this academic year. All credit goes to him who made our project successful. Without his help and contribution our work would not have been able to come to this stage of completeness and fulfilment of our bachelor degree. Apart from him we would like to thank each and every faculty of our **Department of Mechanical & Production Engineering (MPE)** for their knowledge, assistance, motivation and care throughout the study period. We also place on record, our sense of gratitude to one and all, who directly or indirectly, have lent their hands in successful completion of this project work. Finally, we want to express our gratitude to **ALLAH, THE ALMIGHTY**.

# Table of Contents

1	Introduction.....	2
1.1	Wing Geometry .....	4
1.2	Wing Types .....	6
1.3	Construction Materials .....	10
1.4	Airfoil Profile .....	12
1.5	NACA Airfoil Profile .....	13
2	Literature Review .....	15
3	Methodology .....	17
4	Modal Analysis .....	19
4.1	CAD Modelling of Wing.....	19
4.2	Dimensions .....	20
4.3	Material Properties .....	21
4.4	Meshing .....	22
4.5	Boundary Conditions.....	23
4.6	Numerical Results .....	24
5	Experimental Methodology .....	25
5.1	Material Selection.....	25
5.2	Material Properties .....	27
5.3	Construction of The Wing.....	27
5.4	Sensors.....	28
5.5	Maximizing Accuracy .....	30
5.6	Probes .....	31
5.7	Oscilloscope .....	32
5.8	Experimental Setup .....	33
5.9	Final Setup.....	36

5.10	Experimental Results.....	37
6	Mode shapes Using Balsa Wood .....	38
7	Results Comparison .....	39
8	Validation.....	39
9	Variations of Design & Model.....	39
9.1	NACA 4424.....	40
9.2	NACA 4412.....	41
9.3	NACA 2410.....	43
9.4	NACA 16-015 .....	45
9.5	NACA 633-418 .....	47
10	Conclusions.....	49
11	Future Scopes.....	50
12	References.....	50

## List of Figures

Figure 1: Drag and Lift Forces .....	2
Figure 2: General section of an airfoil .....	3
Figure 3: Wing Geometry .....	4
Figure 4: Geometric Twist .....	4
Figure 5: Aspect Ratio .....	5
Figure 6: Dihedral angle.....	5
Figure 7: Different Angles .....	6
Figure 8: Different wing structures .....	7
Figure 9: Rectangular wing.....	7
Figure 10: Tapered wing .....	8
Figure 11: Elliptical wing.....	8
Figure 12: Swept Wing .....	9
Figure 13: Delta Wing.....	10
Figure 14: Flow Chart of Methodology .....	18
Figure 15: NACA 4424 airfoil profile .....	19
Figure 16: Designed aircraft wing.....	20
Figure 17: Mesh .....	22
Figure 18: Zoom view of mesh elements .....	22
Figure 19: Boundary conditions.....	23
Figure 20: Mode Shapes .....	24
Figure 21: Experimental setup .....	25
Figure 22: Eddy-Current Sensor .....	29
Figure 23: Sensor Probe .....	31

Figure 24: Oscilloscope (INSTEK GDS-1102) .....	32
Figure 25: Mounting of Model Wing .....	33
Figure 26: Modified Model Wing .....	34
Figure 27: Mountings .....	35
Figure 28: Full experimental setup .....	36
Figure 29: Experimental Result .....	37
Figure 30: Mode Shapes of Balsa Wood .....	38
Figure 31: Result Comparison .....	39
Figure 32: Frequency vs Mode Graph .....	40
Figure 33: NACA 4412 AIRFOIL PROFILE .....	41
Figure 34: NACA 4412 3D MODEL .....	41
Figure 35: FREQUENCY VS MODE GRAPH .....	42
Figure 36: NACA 2410 AIRFOIL PROFILE .....	43
Figure 37: NACA 2410 3D MODEL .....	43
Figure 38: FREQUENCY VS MODE GRAPH .....	44
Figure 39: NACA 16-015 airfoil profile .....	45
Figure 40: NACA 16-015 3D Model .....	45
Figure 41: FREQUENCY VS MODE GRAPH .....	46
Figure 42: NACA 633-418 AIRFOIL PROFILE .....	47
Figure 43: NACA 633-418 3D Model .....	47
Figure 44: Frequency Vs Mode Graph .....	48



## List of Tables

Table 1: Dimensions of the wing .....	20
Table 2: Elements of Aluminum 2024 T3.....	21
Table 3: Properties of ALUMINUM 2024 T3 .....	21
Table 4: Properties of Balsa wood .....	27
Table 5: Natural Frequencies (Hz).....	40
Table 6: Natural Frequencies (Hz).....	42
Table 7: Natural Frequencies (Hz).....	44
Table 8: Natural Frequencies (Hz).....	46
Table 9: Natural Frequencies (Hz).....	48

---

# ABSTRACT

---

Many studies are being carried out for the design of the wings across the globe by the researchers to strengthen the aircraft wings for steady and sturdy structures for dynamic conditions. The wing design involves its initial considerations and selection of airfoil profile, area of the wing, wing loading characteristics, material and weight of the wing. For initial work, airfoil profile NACA 4424 was selected as root as well as the tip of the wing. This profile along with some specific dimensions was used to design a 3D model in the CAD software SOLIDWORKS 2016. Modal analysis was carried out to find the natural frequencies and mode shapes of the wing using a simulation software COMSOL Multiphysics 5.4 by putting specific boundary conditions and the material properties. A practical model of the wing identical to the simulated 3D model was made using the material Balsa Wood. After experiment using eddy current displacement sensor, similar results were found for the 1<sup>st</sup> natural frequency which did the validation our work. Further, 3D modeling of aircraft wing and modal analysis were done using various airfoil profile like NACA 2410, NACA 4412, NACA 16-015 and NACA 633-015 for design variations like solid model, without ribs and with ribs using the same methodology. These results were compared with one another for determining the best designs of aircrafts for different purposes under different conditions.

# 1 Introduction

---

An airfoil is the cross-section of the wing of a plane. Its main job is to provide lift to the airplane during take-off and while in flight. But, it has also a side effect called drag which opposes the motion of the airplane. The amount of lift needed by a plane depends on the purpose for which it is to be used. Heavier planes require more lift while lighter planes require less lift than the heavier ones. Thus, depending upon the use of airplane, air foil section is determined. Lift force also determines the vertical acceleration of the plane, which in turns depends on the horizontal velocity of the plane[3].

The particular wing design also depends upon many factors like, size, weight, use of the aircraft, desired landing speed, and desired rate of climb. In some aircraft, the larger compartments of the wings are used as fuel tanks. The wings are designated as

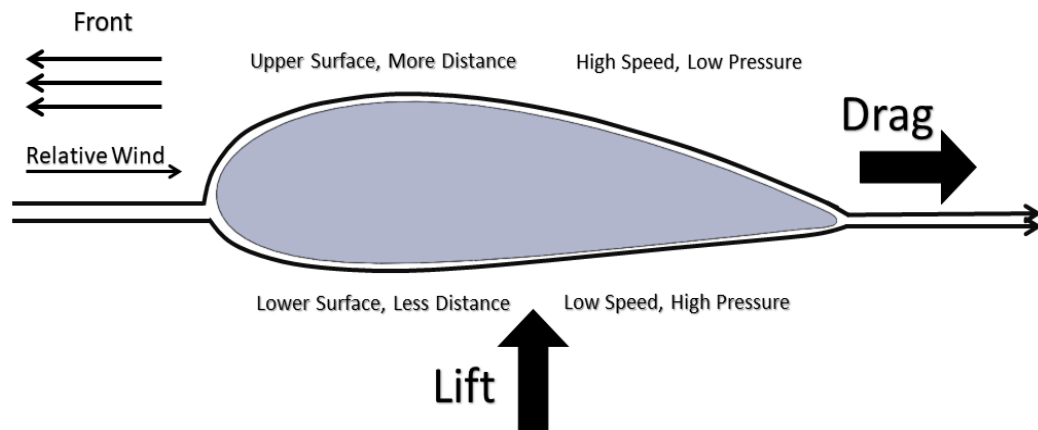


FIGURE 1: DRAG AND LIFT FORCES

right and left, corresponding to the right- and left-hand sides of a pilot seated in the aircraft. An airfoil-formed body travelled through a fluid handles an aerodynamic energy. Subsonic flight airfoils have a trademark shape with an adjusted heading edge, emulated by a sharp trailing edge, regularly with uneven camber. The lift on an airfoil is fundamentally the consequence of its approach and shape. At the point when arranged at a suitable edge, the airfoil diverts the approaching air, bringing about an energy on the airfoil in the heading inverse to the diversion. Most thwart shapes oblige

a positive approach to produce lift; however, cambered airfoils can create lift at zero approach. This turning of the air in the region of the airfoil makes bended streamlines which brings about more level weight on one side and higher weight on the other. This weight contrast is joined by a speed distinction, through Bernoulli's standard, so the ensuing stream field about the airfoil has a higher normal speed on the upper surface than on the more level surface [6].

**Some terms related to airfoil are [17]:**

**Leading edge:** It is the edge of the airfoil facing the direction of motion of plane. It is generally roundish in shape and deflects the air in such a way that the velocity of air on upper surface of the airfoil is more than velocity on the lower surface.

**Trailing edge:** It is the edge of the airfoil which is pointed in nature. It is located at the back side of the airfoil.

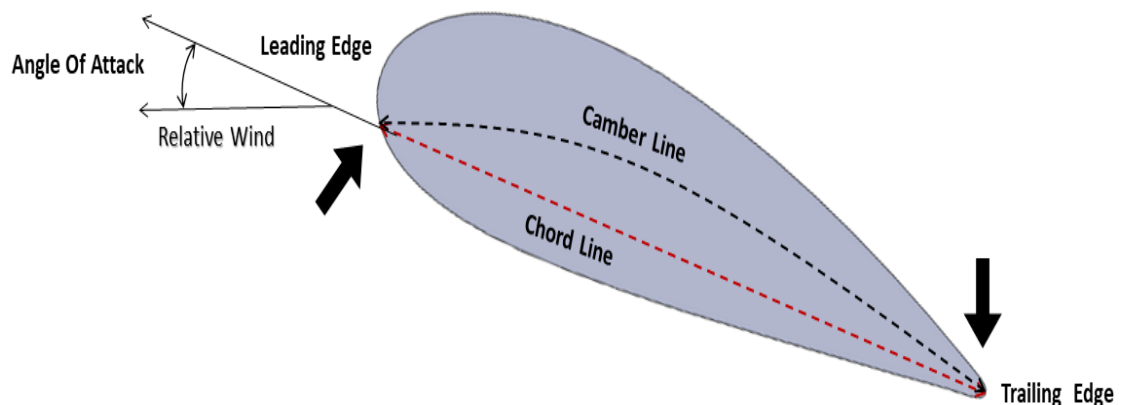


FIGURE 2: GENERAL SECTION OF AN AIRFOIL

**Chord line:** It is a straight line joining the leading edge to the trailing edge. It bisects the airfoil into two parts for a symmetric airfoil but may not do so for an asymmetric airfoil.

**Chamber line:** It is a line joining leading edge and trailing edge and dividing the airfoil into two symmetrical parts. It may or may not be a straight line.

## 1.1 Wing Geometry

**Span:** The distance between to tips is known as Span.

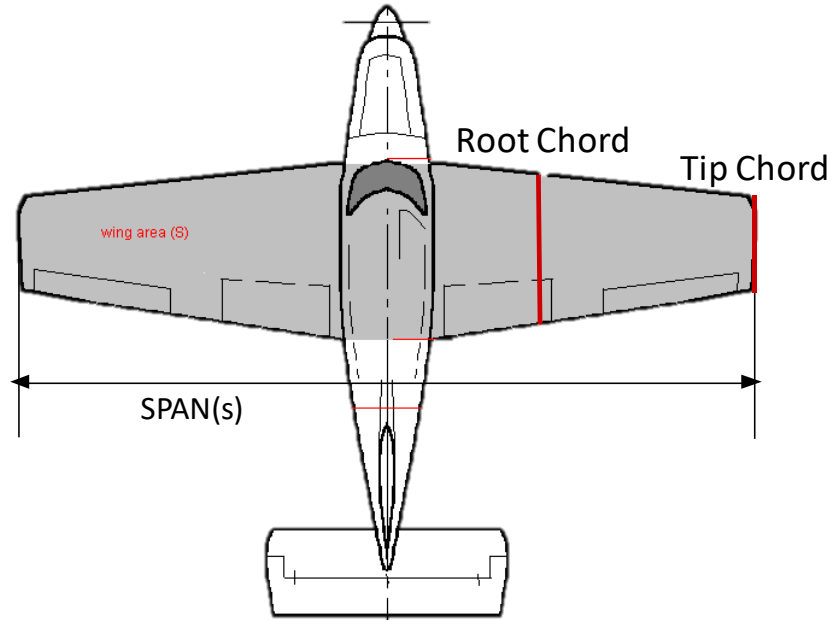


FIGURE 3: WING GEOMETRY [20]

**Geometric twist:** An actual change in the airfoil angle of incidence, usually measured with respect to the root airfoil [17].

- **Wash in** : Angle of incident increases from root to tip  
Tip will stall first
- **Wash out** : Angle of incident decrease from root to tip  
Root will stall first

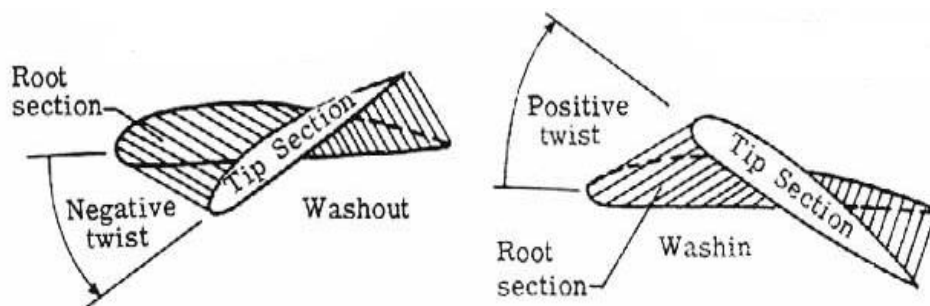


FIGURE 4: GEOMETRIC TWIST [21]

**Aspect ratio:** Aspect ratio is a measure of how long and slender a wing is from tip to tip. The Aspect Ratio of a wing is defined to be the square of the span divided by

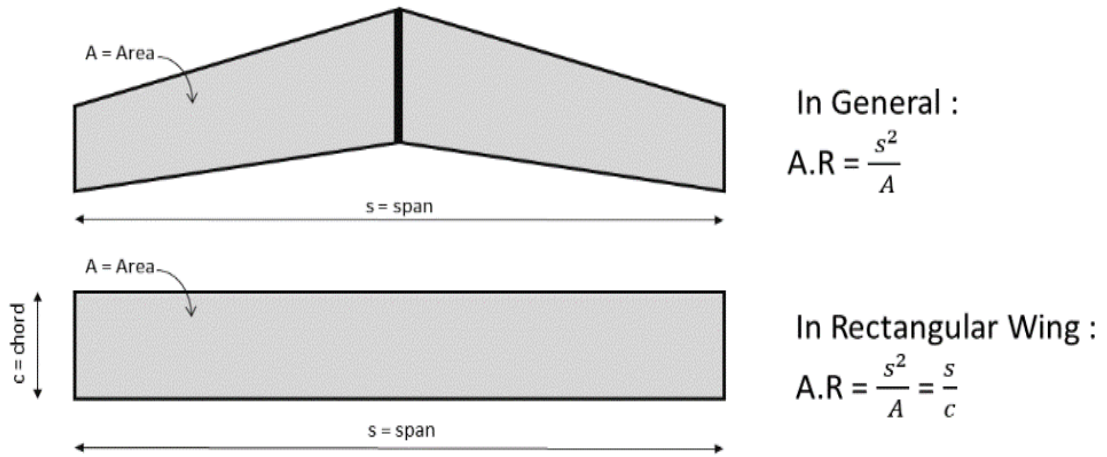


FIGURE 5: ASPECT RATIO [22]

the wing area and is given the symbol AR. For a rectangular wing, this reduces to the ratio of the span to the chord length as shown at the upper right of the figure.

**Dihedral angle:** Dihedral is the upward angle of the wing from the vertical when seen from the front, or nose of the aircraft. If each wing is angled  $5^\circ$  up from the horizontal, then the wing is said to have  $5^\circ$  of dihedral [17].

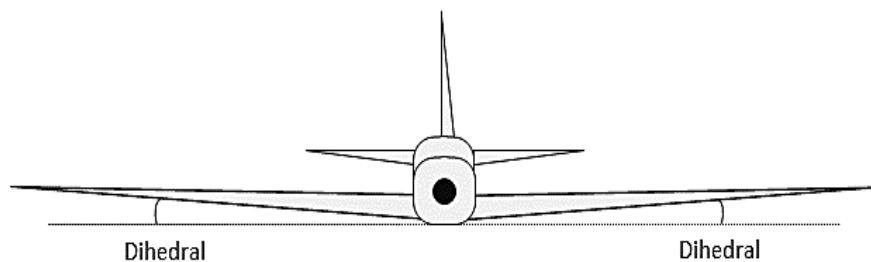


FIGURE 6: DIHEDRAL ANGLE [23]

**Angle of attack:** It is the angle which the chord line makes with the direction of motion of plane. It is an important parameter which affects the coefficient of lift and drag [3].

**Angle of Incidence:** On fixed-wing aircraft, the angle of incidence is the angle between the chord line of the wing where the wing is mounted to the fuselage, and a reference axis along the fuselage [3].

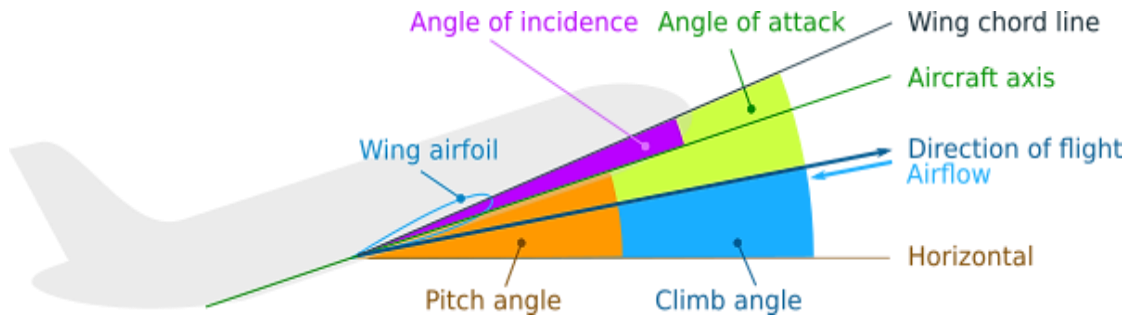


FIGURE 7: DIFFERENT ANGLES [24]

**Thickness Ratio:** It's the ratio of maximum vertical thickness of a wing to its chord length [17].

**Taper Ratio:** Taper ratio is simply the ratio of the chord length of the tip airfoil and the root airfoil chord length [5].

$$\text{Taper ratio} = \frac{\text{Chord length of tip}}{\text{Chord length of the root}}$$

## 1.2 Wing Types

Based on the position of the wing [14]:

- Low wing
- Mid wing
- High wing
- Inverted gull wing
- Gull wing
- Dihedral wing
- Anhedral wing

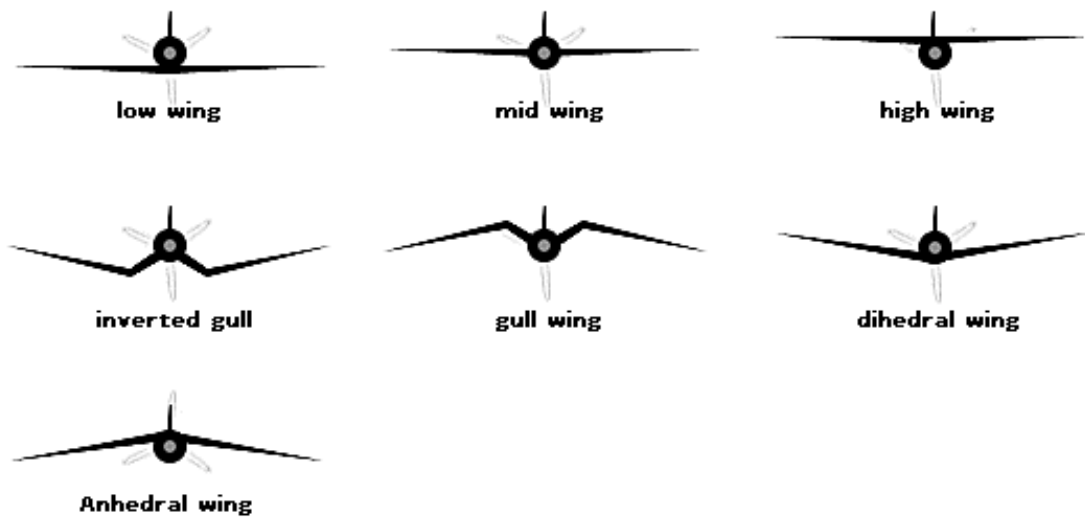


FIGURE 8: DIFFERENT WING STRUCTURES [25]

Based on the shape of the wing [6]:

**Rectangular:** The rectangular wing is the simplest to manufacture. It is a non-tapered, straight wing that is mostly used in small aircrafts. This wing extends out from the aircraft's fuselage at right angles.

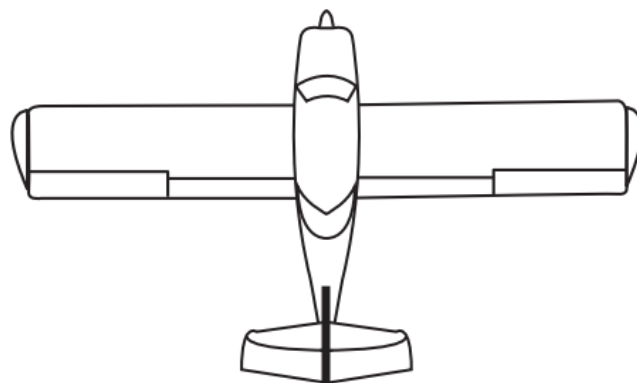


FIGURE 9: RECTANGULAR WING [26]

A good example of an aircraft where a rectangular wing was used is the Piper PA 38. One major disadvantage of a rectangular wing is that it isn't aerodynamically efficient.

**Tapered:** A slightly tapered wing will be more aerodynamically efficient than a rectangular wing. It may be more challenging to build based on the desired taper.



The P-51 Mustang, which was utilized by the USAAF to fight against the Luftwaffe used the tapered wing.

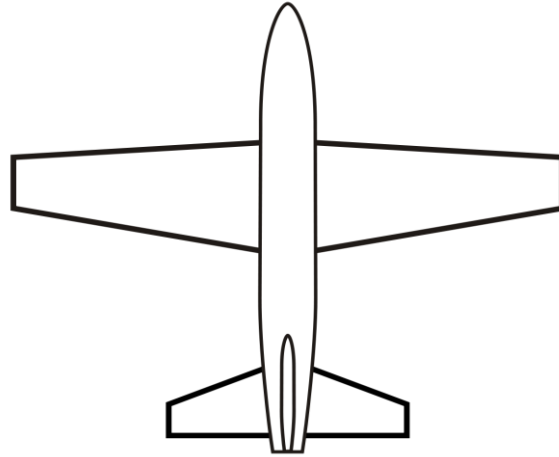


FIGURE 10: TAPERED WING [27]

**Elliptical:** The elliptical wing is aerodynamically most efficient because elliptical spanwise lift distribution induces the lowest possible drag. However, the manufacturability of this aircraft wing is poor. Fabrication is difficult since all ribs are different sizes and do not uniformly change in size. Complex curves will develop on the aircraft skin that will be difficult to cover.

One of the most famous aircrafts in which elliptical wing was used is the Supermarine Spitfire that ruled the skies during the Battle of Britain.

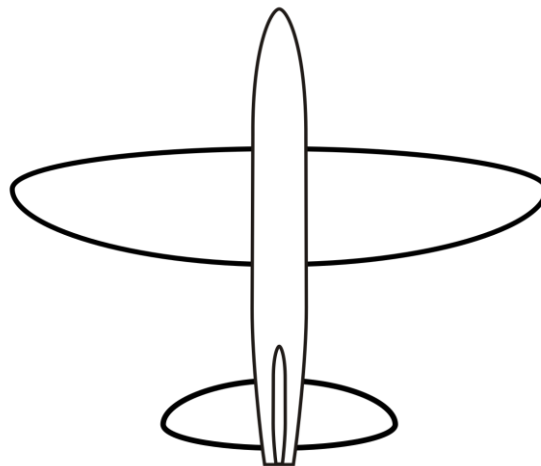


FIGURE 11: ELLIPTICAL WING [28]

**Trapezoid wing:** The trapezoidal wing design offers outstanding flight performance. The trailing edge of the wing sweeps forward while the leading-edge sweeps back. This type of wing is commonly used in U.S. combat aircrafts.

This configuration offers highly efficient supersonic flights and has good stealth characteristics. The only problem is that the wing loading is high which results in reduced maneuverability. The trapezoidal wing is used in the famous F-22 Raptor jet.

**Swept wing-** A swept wing is a wing that angles either backward or occasionally forward from its root rather than in a straight sideways direction. The majority of high-speed commercial aircrafts use swept back wings. Boeing 787 Dreamliner is one example out of many that uses swept back wings.

The Sukoi Su-47 Berkut is one of the very few aircraft that used swept backward wing.

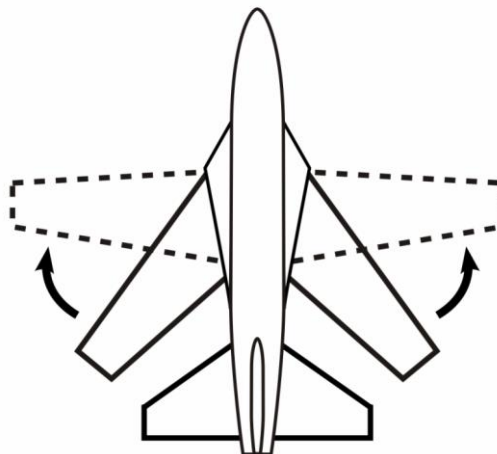


FIGURE 12: SWEPT WING [29]

**Delta wing-** The delta wing doesn't just offer efficient flight experience but is also strong structurally and provides large volume for fuel storage. This wing is also simple to manufacture and maintain.

The Dassault Mirage 2000 is a prime example of an aircraft which uses tailless delta wings. Some aircrafts use tailed delta wings and one of the most famous of those aircrafts is the Russian MiG-21.

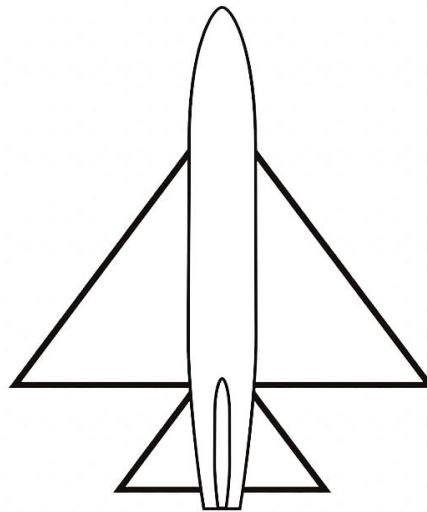


FIGURE 13: DELTA WING [30]

### 1.3 Construction Materials

An aircraft must be constructed of materials that are both light and strong. Early aircraft were made of wood. Lightweight metal alloys with a strength greater than wood were developed and used on later aircraft. Materials currently used in aircraft construction are classified as either metallic materials or nonmetallic materials [35].

#### **Metallic Materials**

The most common metals used in aircraft construction are aluminum, magnesium, titanium, steel, and their alloys.

#### **Alloys**

An alloy is composed of two or more metals. The metal present in the alloy in the largest amount is called the *base metal*. All other metals added to the base metal are called *alloying elements*. Adding the alloying elements may result in a change in the properties of the base metal. For example, pure aluminum is relatively soft and weak. However, adding small amounts of copper, manganese, and magnesium will increase aluminum's strength many times. Heat treatment can increase or decrease an alloy's strength and hardness. Alloys are important to the aircraft industry. They provide materials with properties that pure metals do not possess.

## **Aluminum**

Aluminum alloys are widely used in modern aircraft construction. Aluminum alloys are valuable because they have a high strength-to-weight ratio. Aluminum alloys are corrosion resistant and comparatively easy to fabricate. The outstanding characteristic of aluminum is its lightweight.

## **Magnesium**

Magnesium is the world's lightest structural metal. It is a silvery-white material that weighs two-thirds as much as aluminum. Magnesium is used to make helicopters. Magnesium's low resistance to corrosion has limited its use in conventional aircraft.

## **Titanium**

Titanium is a lightweight, strong, corrosion resistant metal. Recent developments make titanium ideal for applications where aluminum alloys are too weak and stainless steel is too heavy. Additionally, titanium is unaffected by long exposure to seawater and marine atmosphere. Steel Alloys Alloy steels used in aircraft construction have great strength, more so than other fields of engineering would require. These materials must withstand the forces that occur on today's modern aircraft. These steels contain small percentages of carbon, nickel, chromium, vanadium, and molybdenum. High-tensile steels will stand stress of 50 to 150 tons per square inch without failing. Such steels are made into tubes, rods, and wires. Another type of steel used extensively is stainless steel. Stainless steel resists corrosion and is particularly valuable for use in or near water.

## **Nonmetallic Materials**

In addition to metals, various types of plastic materials are found in aircraft construction. Some of these plastics include transparent plastic, reinforced plastic, composite, and carbon-fiber materials.

### **Transparent Plastic**

Transparent plastic is used in canopies, windshields, and other transparent enclosures. You need to handle transparent plastic surfaces carefully because they are

relatively soft and scratch easily. At approximately 225°F, transparent plastic becomes soft and pliable.

### **Reinforced Plastic**

Reinforced plastic is used in the construction of wingtips, stabilizer tips, antenna covers, and flight controls. Reinforced plastic has a high strength-to-weight ratio and is resistant to mildew and rot. Because it is easy to fabricate, it is equally suitable for other parts of the aircraft. Reinforced plastic is a sandwich-type material. It is made up of two outer facings and a center layer. The facings are made up of several layers of glass cloth, bonded together with a liquid resin. The core material (center layer) consists of a honeycomb structure made of glass cloth. Reinforced plastic is fabricated into a variety of cell sizes.

### **Composite and Carbon Fiber**

High-performance aircraft require an extra high strength-to-weight ratio material. Fabrication of composite materials satisfies this special requirement. Composite materials are constructed by using several layers of bonding materials (graphite epoxy or boron epoxy). These materials are mechanically fastened to conventional substructures. Another type of composite construction consists of thin graphite epoxy skins bonded to an aluminum honeycomb core. Carbon fiber is extremely strong, thin fiber made by heating synthetic fibers, such as rayon, until charred, and then layering in cross sections.

## **1.4 Airfoil Profile**

There are different types of airfoil profile available for aircraft wing design. For example – NACA, ARA, CLARK, DESA, DAVIS, RAE, RAF & etc. We worked with NACA airfoil profile. The advantages of NACA airfoils are as follows [36] –

- Good stall characteristics
- Small center of pressure movement across large speed range
- Higher maximum lift coefficient
- Low pitching moment
- Optimized for high speed

## 1.5 NACA Airfoil Profile

The early NACA airfoil series, the 4-digit, 5-digit, and modified 4-/5-digit, were generated using analytical equations that describe the camber (curvature) of the mean-line (geometric centerline) of the airfoil section as well as the section's thickness distribution along the length of the airfoil. Later families, including the 6-Series, are more complicated shapes derived using theoretical rather than geometrical methods. Before the National Advisory Committee for Aeronautic (NACA) developed these series, airfoil design was rather arbitrary with nothing to guide the designer except past experience with known shapes and experimentation with modifications to those shapes [35].

### **NACA Four-Digit Series:**

The first family of airfoils designed using this approach became known as the NACA Four-Digit Series. The first digit specifies the maximum camber ( $m$ ) in percentage of the chord (airfoil length), the second indicates the position of the maximum camber ( $p$ ) in tenths of chord and the last two numbers provide the maximum thickness ( $t$ ) of the airfoil in percentage of chord. For example, the NACA 2415 airfoil has a maximum thickness of 15% with a camber of 2% located 40% back from the airfoil leading edge (or  $0.4c$ ) [35].

### **NACA Five-Digit Series:**

The NACA Five-Digit Series uses the same thickness forms as the Four-Digit Series but the mean camber line is defined differently and the naming convention is a bit more complex. The first digit, when multiplied by  $3/2$ , yields the design lift coefficient ( $c_l$ ) in tenths. The next two digits, when divided by 2, give the position of the maximum camber ( $p$ ) in tenths of chord. The final two digits again indicate the maximum thickness ( $t$ ) in percentage of chord. For example, the NACA 23012 has a maximum thickness of 12%, a design lift coefficient of 0.3, and a maximum camber located 15% back from the leading edge [35].

### **Modified NACA Four- and Five-Digit Series:**

The airfoil sections you mention for the B-58 bomber are members of the Four-Digit Series, but the names are slightly different as these shapes have been modified. Let us consider the root section, the NACA 0003.46-64.069, as an example. The basic shape is the 0003, a 3% thick airfoil with 0% camber. This shape is a symmetrical airfoil that is identical above and below the mean camber line. The first modification we will consider is the 0003-64. The first digit following the dash refers to the roundedness of the nose. A value of 6 indicates that the nose radius is the same as the original airfoil while a value of 0 indicates a sharp leading edge. Increasing this value specifies an increasingly more rounded nose. The second digit determines the location of maximum thickness in tenths of chord. The default location for all four- and five-digit airfoils is 30% back from the leading edge. In this example, the location of maximum thickness has been moved back to 40% chord. Finally, notice that the 0003.46-64.069 features two sets of digits preceded by decimals. These merely indicate slight adjustments to the maximum thickness and location thereof. Instead of being 3% thick, this airfoil is 3.46% thick. Instead of the maximum thickness being located at 40% chord, the position on this airfoil is at 40.69% chord [35].

### **NACA 6-Series:**

Although NACA experimented with approximate theoretical methods that produced the 2-Series through the 5-Series, none of these approaches was found to accurately produce the desired airfoil behavior. The 6-Series was derived using an improved theoretical method that, like the 1-Series, relied on specifying the desired pressure distribution and employed advanced mathematics to derive the required geometrical shape. The goal of this approach was to design airfoils that maximized the region over which the airflow remains laminar. In so doing, the drag over a small range of lift coefficients can be substantially reduced. The naming convention of the 6-Series is by far the most confusing of any of the families discussed thus far, especially since many different variations exist. One of the more common examples is the NACA 641-212,  $a=0.6$ . In this example, 6 denotes the series and indicates that this family is designed for greater laminar flow than the Four- or Five-Digit Series. The second digit, 4, is the location of the minimum pressure in tenths of chord (0.4c). The subscript 1

indicates that low drag is maintained at lift coefficients 0.1 above and below the design lift coefficient (0.2) specified by the first digit after the dash in tenths. The final two digits specify the thickness in percentage of chord, 12%. The fraction specified by 'a' indicates the percentage of the airfoil chord over which the pressure distribution on the airfoil is uniform, 60% chord in this case. If not specified, the quantity is assumed to be 1, or the distribution is constant over the entire airfoil [35].

## 2 Literature Review

---

To claim our objectives and to find out new scopes for any new method of design or to do some modifications a literature survey is done over the researchers concerned with the detailed study of aircraft wing. Fundamental properties like vibration which has an important impact on failure of the structure is desired to explore by this literature survey.

**Kakumani Sureka and R Satya Meher** in their paper they modelled A300 aircraft wing using standard NACA 64215 airfoil with spars and ribs digitally using different materials. They arrived to the conclusion that Aluminum alloy 7068 is preferred over Aluminum alloy in order to give the more strength to the structure. [2]

**K. Sruthi, T. Lakshmana Kishore, M. Komaleswara Rao** in their paper conclude that the difference between the values of deformation, equivalent stress, max principle stress, stress intensity and shear stress with Al alloy and Aluminum + Silicon Carbide are minimal. The results obtained are optimum. As the difference between the two result values are minimal. We can use aluminum + Silicon carbide instead of using aluminum alloy in order to give the more strength to the structure. The effect of pressure during take-off condition is more for Aluminum and less for Al + SiC which is strongest and light weight, and also reduces the weight of the wing. Thus, we can conclude that at the above assumed loading conditions and constraints flight wing structure will not fail due to material properties. We can conclude that aluminum + silicon carbide can be replaced with aluminum alloy. [3]



**Avnish Kumar** in his “Investigation of airfoil design.” Said that Lift coefficient was found to be higher for Asymmetric airfoil than the Symmetric airfoil for same chord length and maximum camber of the airfoil at same angle of attack. [4]

**Aswani Kodali** and T.N. Charyulu in their paper with the title “modeling and analysis on wing of A380 flight” conducted structural & thermal analysis on AIR BUS A380 wing to calculate the stress, strain & thermal flux for finding the wing to be safe. For simulation and modeling they used software like CATIA for determining model for analysis FEA package ANSYS. In their simulation the obtained stress and strain values were within the limiting range. The maximum stresses that wing of a flight can with stand are 700pa. But obtained stress was 400pa. [5]

**P. JEEVANANTHAM, L. MANIKUMAR** in their paper dealt with the structural design and flow analysis of M wing in an aircraft. The wing design involves its initial considerations and selection of airfoil, area of the wing, wing loading characteristic and weight of the wing. Their design proved to be viable by the results that they obtained from the virtual flow analysis of the wing analyzed by the Design-Foils tool test results. [6]

**Dr. R. Rajappan, & V. Pugazhenth**i dealt in their papers with bending Finite Element Analysis of monocoque laminated composite aircraft (subsonic and supersonic) wing using commercial software ANSYS. They used NACA 4412 as model. They concluded that wing model was severely affected by the loads on along wing direction, across wing direction, vertical direction. Von misses stress was calculated in order to know the maximum stress levels and minimum stress levels on the wing. [7]

**Nikhil A. Khadse & Prof. S. R. Zaweri** in their paper presents modal analysis of aircraft wing. Aircraft wing used for investigation is A300 (wing structure consist of NACA 64A215). A cad model of an aircraft wing has been developed using modeling software PROE5.0 and modal analysis was carried out by using ANSYS WORKBENCH14.0. modal analysis has been carried out by fixing one end (root chord) of aircraft wing while another end (tip chord) is free. They also used a cantilever beam modal analysis for validation of the simulation of the airfoil. This investigation revealed that natural frequency obtained from numerical and theoretical approach were

in close agreement, which validated FE model of the cantilever beam for modal analysis. [8]

**T. Gultop** studied the impact of perspective degree on Airfoil performance. The reason for this study was to focus the ripple conditions not to be kept up throughout wind tunnel tests. These studies indicate that aeroelastic insecurities for the changing arrangements acknowledged showed up at Mach number 0.55, which was higher than the wind tunnel Mach number point of confinement velocity of 0.3. [9]

**Lica Flore and Albert Arnau Cubillo** presented the results of the dynamical behavior on an aircraft wing structure. The study has consisted strain gauges to test aircraft wing dynamically in which the vibration parameters of the structure have been determined. [10]

**Dr. M. Neubauer, G. Gunther** gave description regarding various loads to be considered in the analysis and design of air frame structures. He also discussed the Conversion of "external loads" into structural airframe loads. He conducted aircraft analysis using static loads and fatigue loads [11].

### 3 Methodology

---

The 3D design of the wing was prepared using SOLIDWORKS 2016. Finite element analysis was applied to further our understanding of the mechanics of the wing. Finite element methods had been used by many researchers to aid the process of development of wing structure [2]. For the purpose of simplifying the analysis we considered the wing as a cantilever beam. The design was then imported to COMSOL Multiphysics 5.4. Using modal analysis, the natural frequencies and corresponding mode shapes were found. An experimental setup was made with the same design of wing and tested in the same environment created in the lab. An eddy current sensor was used to take the readings of natural vibration and the output was shown in the oscilloscope. These results were compared to validate our research work. For further modifications, different naca airfoil profiles were selected. Mode shapes and natural frequencies were found through modal analysis for different structures. We used 3

types of structures here- solid, without ribs and with ribs. These results were compared further.

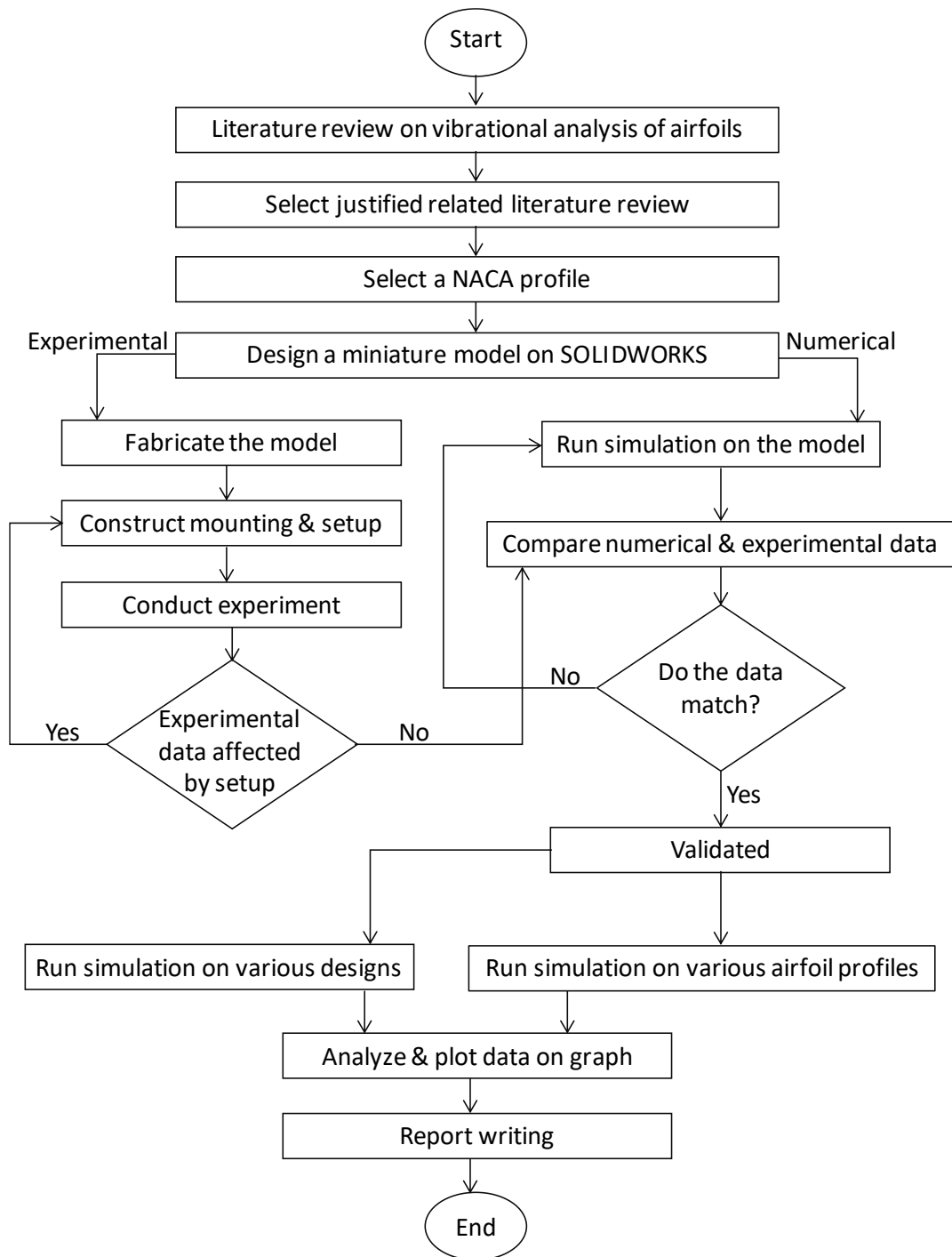


FIGURE 14: FLOW CHART OF METHODOLOGY

## 4 Modal Analysis

---

The modal analysis is a common method used to investigate dynamical behaviors of mechanical structures under the dynamic excitation. It is used to determine the dynamic characteristics of a system such as natural frequency, mode shapes etc. Emitted noise reduction from the system to the environment is enabled by the modal analysis. It helps finding out the reasons of vibrations which cause damage on the system and used for reducing it. In short, one can improve the performance of a system by using modal analysis method. Two primarily known methods of modal analysis are the numerical modal analysis and the experimental modal analysis [12].

### 4.1 CAD Modelling of Wing

The solid model of aircraft wing is made using SOLIDWORKS 2016.

Steps to generate the model:

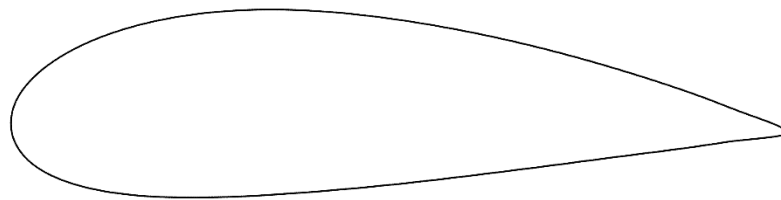


**FIGURE 15: NACA 4424 AIRFOIL PROFILE**

- First by plotting coordinates collected from the NACA profile standards. [12]
- Creating splines making the shape of the airfoils at the tip & root of the wing with proper dimensions.
- Using Loft feature generating of the aircraft wing.

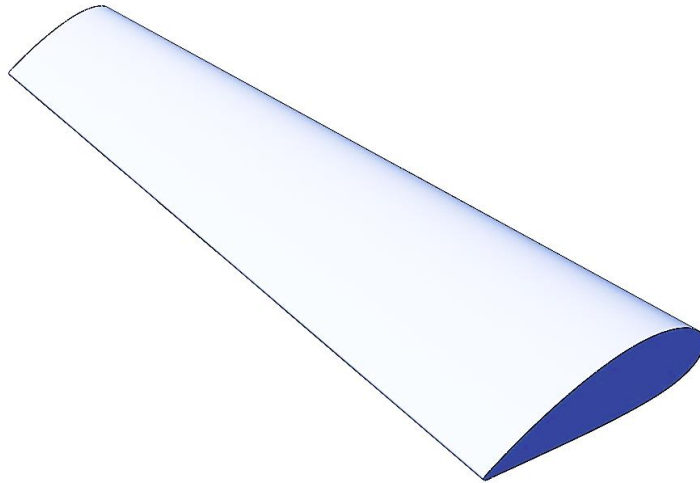


**FIGURE 16: DESIGNED AIRCRAFT WING**

## 4.2 Dimensions

Wing length : 1m  
Chord length : Root - 0.397 m  
Tip - 0.1756 m  
Thickness of the surface taken: 3 mm

**TABLE 1: DIMENSIONS OF THE WING [2]**

Geometric Twist (DEG)	1.5 Degrees
Incidence Angle (DEG)	2.5 Degrees
Dihedral Angle (DEG)	5.5 Degrees
Aspect Ratio	7.448
Taper Ratio	2.271

### 4.3 Material Properties

Material Name - ALUMINUM 2024 T3

**TABLE 2: ELEMENTS OF ALUMINUM 2024 T3 [31]**

<b>Elements</b>	<b>Weight %</b>
Al	90.7-94.7
Cr	max 0.1
Cu	3.8-4.9
Fe	max 0.5

**TABLE 3: PROPERTIES OF ALUMINUM 2024 T3 [31]**

<b>Properties</b>	<b>Values</b>
Elastic (Young's, Tensile) Modulus	73 GPa
Poisson's Ratio	0.33
Tensile Strength: Ultimate (UTS)	345 MPa
Thermal Conductivity	121 W/m-K
Density	2750 kg/m <sup>3</sup>
Shear Strength	283 MPa

## 4.4 Meshing

Unit cell size of a mesh is very important. The accuracy of the result of the experiment depends on the element size of the mesh. Finer element size enhances the



**FIGURE 17: MESH**

precision of the result, but this requires higher computing power and consumes more time. As the total number of nodes increases with the increase of total number of element size, the simulation requires to solve all those points. Keeping the computing power of the computer used, the mesh was generated. Here,

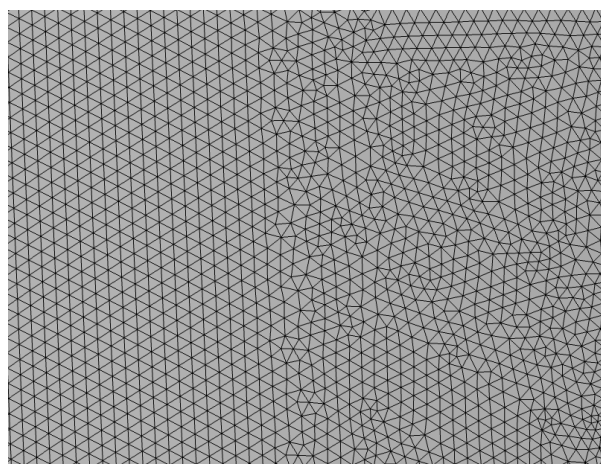


**FIGURE 18: ZOOM VIEW OF MESH ELEMENTS**

**Element size parameters:**

Maximum element size	: 0.012 m
Minimum element size	: 0.002 m
Maximum element growth rate	: 1.5
Curvature factor	: 0.5
Resolution of narrow regions	: 0.8

**This generates:**

Number of domain elements	: 147863
Number of boundary elements	: 17116
Number of edge elements	: 294

This provides an acceptable accuracy of result consuming a moderate computation time.

## 4.5 Boundary Conditions

At the Root of the wing, frictionless fixed support was given similar to a cantilever beam which is marked blue in the figure 19. Frictionless support places a normal constraint on the entire surface. Transitional displacement was allowed in all directions.

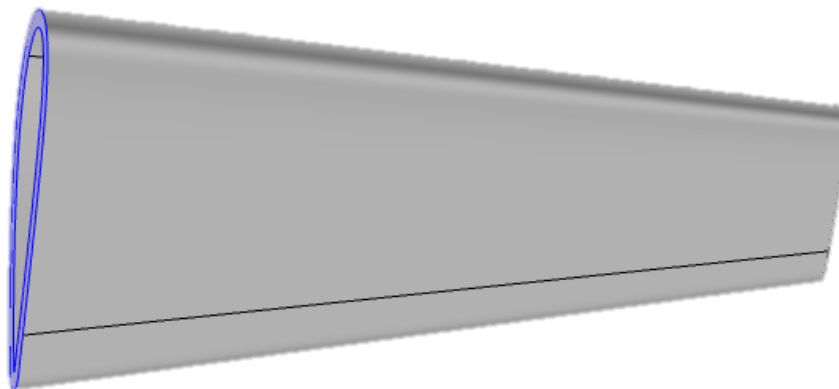


**FIGURE 19: BOUNDARY CONDITIONS**



## 4.6 Numerical Results

While running the simulation we set the analysis settings to find the 6 natural frequencies and their corresponding mode shapes. The results are shown below:

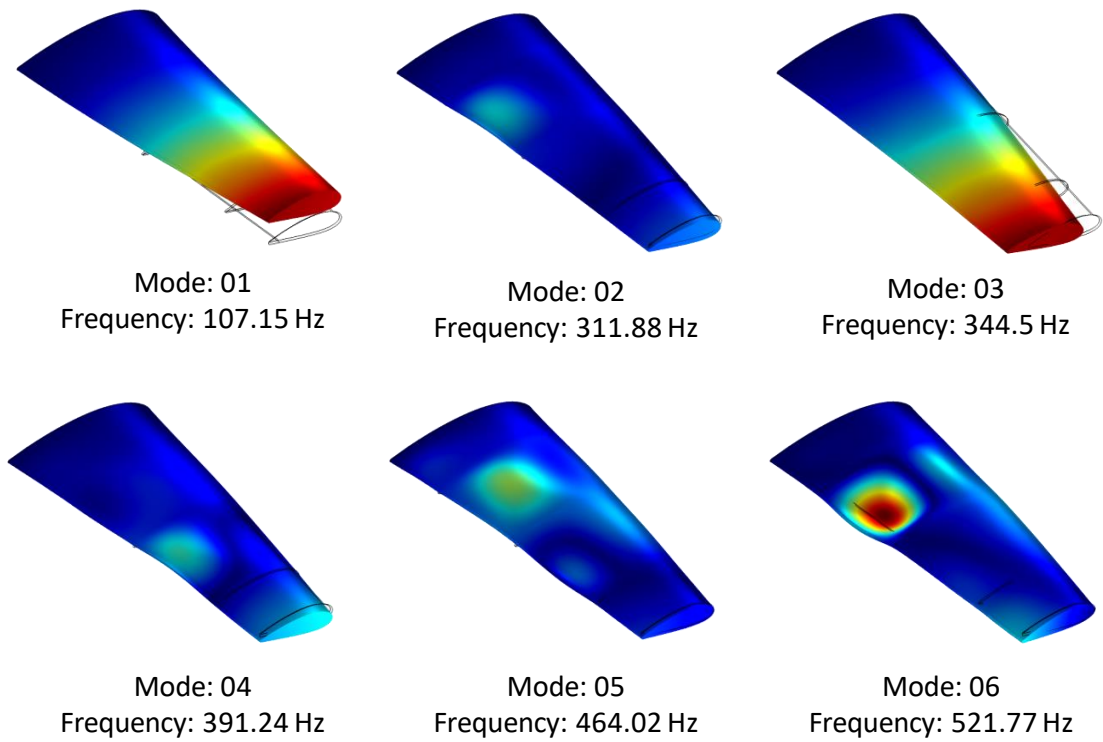


FIGURE 20: MODE SHAPES

## 5 Experimental Methodology

---

A setup was made to conduct an experiment to find the natural frequencies. It consists:

- A wing
- An Eddy Current Sensor
- A probe
- An Oscilloscope
- Wires
- Aluminum Stripes

Here is the schematic diagram of the experimental setup:

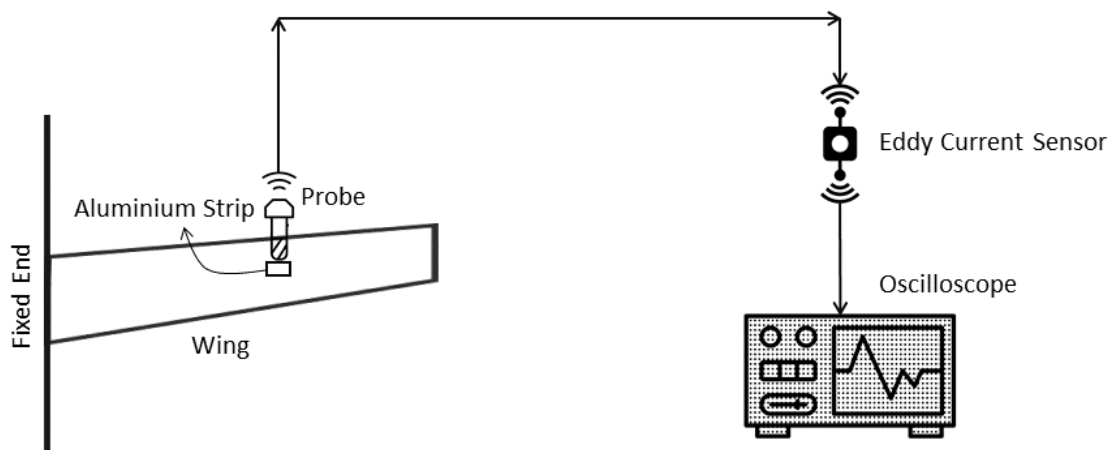


FIGURE 21: EXPERIMENTAL SETUP

### 5.1 Material Selection

Materials that were considered for the construction of the model are [18]:

**Composite:** Constructed from materials such as carbon fiber, Kevlar, or fiberglass this allows for very strong and very light wing to be fabricated. However, the time and cost to produce a one of a kind wings can be restrictive. Furthermore, this technique will require specialized tools and processes for constructing molds and parts. Nowadays, one of the more favored materials for this purpose is carbon fiber. In many

wings, carbon fiber has been used and it actually gives a better shape to the plane as a whole.

**Traditional wooden:** Requires only basic tools for a basic airplane. Material cost can be reduced along with time since the material is easy to work with and commonly available. Additionally, since the required techniques have been used for many years an abundance of information exists on the subject from build to covering the model.

**Foam:** Fast to build and durable, however the wing is generally heavier since the foam requires substantial reinforcements to be able to withstand the loads applied during experiment.

Some of the most commonly used materials for creating such models are: extruded polystyrene foam also known as Styrofoam or expanded polystyrene. These are easily available materials and, of course, they are affordable.

**Depron:** Depron is another material that is in demand for making the wing. The reason most people are opting for this material is its ability to mix flexibility along with rigidity which is not something that you get in common wing materials.

**Balsa Wood:** Balsa has its own strengths and weaknesses, and for most cases, is compressed along the grain. It highly contrasts foam in that it can hold its shape longer for lower diameter pieces and can be used as a slight replacement for string in a wing design. Other materials fall apart in both cases. The lightness of the material makes up for its weakness.

Considering the material availability, cost, and demand of the project we decided to go with the 'Balsa Wood'. The 'Balsa Wood' allowed the model to be tapered very easily. Also, it was easy to mount and it withstood the forces applied from the mountings of the experiment and held its shape.

## 5.2 Material Properties

**TABLE 4: PROPERTIES OF BALSA WOOD [32]**

<b>Properties</b>	<b>Values</b>
Elastic (Young's, Tensile) Modulus	3.0 GPa
Poisson's Ratio	0.38
Tensile Strength: Ultimate (UTS)	14 MPa
Thermal Conductivity	0.1 W/m-K
Density	0.13 g/cm <sup>3</sup>
Compressive (Crushing) Strength	7.0 MPa

## 5.3 Construction of The Wing

Hot wire cutting method was used for the fabrication of the model. A hot wire cutter is an electrical tool used to cut polystyrene, foams and similar materials. The device consists of a thin, taut cutting wire, often made of Nichrome, Titanium, Stainless steel, or a thicker wire preformed into a desired shape, which is heated via electrical resistance to approximately 500°C. As the cutting wire is passed through the material to be cut, the heat from the wire vaporizes the material just in advance of contact. We have used a hot wire cutter of 12V and 600mA with Nichrome wire for cutting the Balsa Wood. Arguably, the most important part of the entire wing has to be the frame. For achieving the tapered shape, we have used a total of Eleven Balsa Wood pieces of varying curvature for the frame. The entire frame is one-meter-long and is constructed with Balsa Wood of 5mm thickness. Two long horizontal Balsa Wood pieces are used to support the entire inner frame. The frame is then covered with Balsa Wood of 2mm thickness for its flexibility. While fabricating the model wing the actual tapered shape of the NACA-4424 airfoil was maintained as much as possible.

Hot epoxy glue and normal wooden glue were used for the fabrication. The wing is made lightweight so it doesn't bend by its own weight while kept mounted on experiment setup. This type of fabrication was chosen over other processes such as 3D



Fig: Fabrication of The Wing

printing because, 3D printing for such a dimension is not easily available. The material used to 3D print the wing leaves a rough finish on the wing surface compared to the smooth finish of 'Balsa Wood' fabrication. Also, the lightest material (e.g. - ABS Plastic) available for 3D printing such a model is quite heavier than the 'Balsa Wood' wing, as a result the 3D printed wing could have sustained damage to its mounting points on the experimental setup due to its own weight.

## 5.4 Sensors

For measuring the natural frequency of the model wing Eddy Current Displacement Sensor have been used [15].

**Eddy Current Sensor:** Lion Precision ECL202 Eddy-Current Displacement Sensor is used for the experiment. This specific model was chosen because it provides high-resolution, noncontact measurement of position changes of a conductive target. The system consists of driver electronics and a probe calibrated for a specific material and range. The ECL202 provides a linear analog voltage proportional to changes in

the model wing's position and a digital switched (set point) output with a user programmed switching set point.

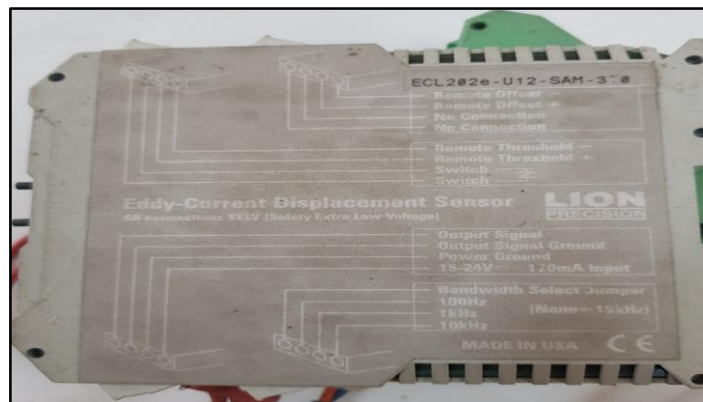


FIGURE 22: EDDY-CURRENT SENSOR

The eddy-current sensor produces an alternating magnetic field at the probe tip. When this field is near a conductive material, the field creates (induces) small electrical eddy-currents in the material. These currents generate a magnetic field that opposes the field from the sensor. As the gap between the probe and target gets smaller, the field interaction changes. The sensor electronics measure this field interaction and generate an output voltage proportional to the change in the gap [16].

The Sensor consists of the following features:

- Ranges from 0.25 mm to 15 mm
- Industry standard 0-10 VDC Output
- Set point Contacts Output
- CE Compliant
- Linearity: 0.2%
- Typical resolution-
  - Nonferrous: 15 kHz - 0.007%; 100 Hz - 0.002%
  - Ferrous: 15 kHz - 0.009%; 100 Hz - 0.003%
- Probe can be used in wet, dirty environments
- Push-Button Offset
- Push-Button Switch Threshold (Set point)
- Range Indicating LEDs
- Remote Offset and Threshold Activation

- User-Selectable
- Bandwidth/Resolution 100 Hz, 1 kHz, 10 kHz, 15 kHz

## 5.5 Maximizing Accuracy

Accuracy at the high resolutions created by the precision eddy-current sensors may have been affected by the environment and measurement setup. So, target areas were at least three times larger than the probe diameter. Probes was positioned in a stable mechanical system in a stable environment. Even small changes in temperature cause expansions of the target that are detectable by the sensor. But the magnetic fields of the eddy-current sensor do not “see” nonconductive materials and therefore are not affected by most contaminants. This allows the eddy-current sensor to operate while immersed in liquids and in the presence of machine coolants or other liquid materials present in the sensing area. We had used this feature of the eddy-current sensor to our advantage. As our model wing is made of Balsa Wood which is a nonconductive material, it could have affected the accuracy of the sensor [16].

To measure the natural frequency of the model wing, small cut outs of Aluminum was placed on the surface of the wing. This was done because the eddy-current sensor reacts to conductive materials only. So, even though Balsa Wood being nonconductive was helped with increasing the accuracy of the experiment it created the problem of not getting any values at all. This problem was overcome with the placement of Aluminum cut outs without sacrificing any accuracy.

The eddy-currents induced in the target material are dependent on the material’s properties of permeability and resistivity. As a result, eddy-current sensors are sensitive to changes in material. There can be a drastic difference between magnetic (iron, steel) and nonmagnetic (aluminum, copper) materials. Less drastic, but still significant, is the difference between two nonmagnetic materials. The material and alloy must be specified with orders to assure an accurate calibration. Because the magnetic fields penetrate the surface of the target, target materials have minimum thickness requirements; this varies with material type. So, to avoid this kind of errors in values obtained, we have only used Aluminum as our target material.

## 5.6 Probes

Cable length is three meters. Extension cable length was measured from end-to-end including connectors. Standard temperature probe cables have PUR jackets. High-Temperature probes use PTFE. For our experiment we have used armored cabled probe. Armored cable is available on probes 12 mm (U12) and larger. The armor is only affixed at the probe end. Probe was mounted to avoid interaction between the sensing



FIGURE 23: SENSOR PROBE [33]

field and the mounting hardware. The area within 3 probe diameters to the sides and 1.5 diameters behind was kept clear of any metallic objects other than the object to be measured [15].

Also ungrounded targets have the potential to inject noise into the sensor. If the output is unusually noisy, so the target should be grounded. But Balsa wood being nonconductive and the Aluminum cut outs having no other metal or magnetic field around it helped with keeping the noise at a minimum.



## 5.7 Oscilloscope

An 'oscilloscope', previously called an 'oscillograph', and informally known as a scope or o-scope, CRO (for cathode-ray oscilloscope), or DSO (for the more modern digital storage oscilloscope), is a type of electronic test instrument that graphically displays varying signal voltages, usually as a two-dimensional plot of one or more signals as a function of time. Other signals (such as sound or vibration) can be converted to voltages and displayed [37].

Oscilloscopes display the change of an electrical signal over time, with voltage and time as the Y- and X-axes, respectively, on a calibrated scale. The waveform can then

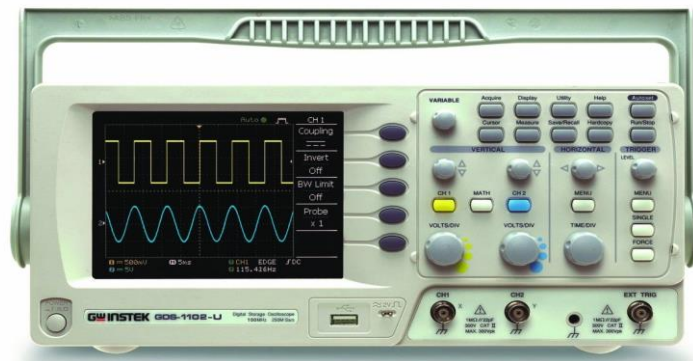


FIGURE 24: OSCILLOSCOPE (INSTEK GDS-1102) [34]

be analyzed for properties such as amplitude, frequency, rise time, time interval, distortion, and others. Modern digital instruments may calculate and display these properties directly. Originally, calculation of these values required manually measuring the waveform against the scales built into the screen of the instrument.

The oscilloscope can be adjusted so that repetitive signals can be observed as a continuous shape on the screen. A storage oscilloscope can capture a single event and display it continuously, so the user can observe events that would otherwise appear too briefly to see directly.

Oscilloscopes are used in the sciences, medicine, engineering, automotive and the telecommunications industry. General-purpose instruments are used for maintenance of electronic equipment and laboratory work. Special-purpose oscilloscopes may be

used for such purposes as analyzing an automotive ignition system or to display the waveform of the heartbeat as an electrocardiogram.

Early oscilloscopes used cathode ray tubes (CRTs) as their display element (hence they were commonly referred to as CROs) and linear amplifiers for signal processing. Storage oscilloscopes used special storage CRTs to maintain a steady display of a single brief signal. CROs were later largely superseded by digital storage oscilloscopes (DSOs) with thin panel displays, fast analog-to-digital converters and digital signal processors. DSOs without integrated displays (sometimes known as digitizers) are available at lower cost and use a general-purpose digital computer to process and display waveforms.

Instek GDS-1102 is used in our experimental setup to take the readings from the sensor.

## 5.8 Experimental Setup

### **Initial**

For conducting the experiment, we had to consider the actual positioning and mounting of a wing on an Airplane. Keeping this in mind we came up with a simpler version of wing mounting that is able to produce the same result as an actual airplane



FIGURE 25: MOUNTING OF MODEL WING

wing mounting. The main objective was to fix the wider end of the model wing. And to do that we have used two metal clamps. These two clamps exert just enough pressure to the wide end of the model wing to keep it fixed without causing any damage to it.

The next step of the experiment was to mount the sensors. The probe of the sensors was mounted on a metal stand. The probe is not fixed on the stand, its position can easily be switched and manipulated for more accurate results.

### **Modifications**

The initial experimental setup produced quite a few errors which led to the modification of the setup. The major problems that were faced after performing the experiments:

- Lack of precision resulted in random data
- Noise due to the lack of dampening from the mounting
- Joints of the model wing could not withstand the boundary conditions applied

To produce better and acceptable results the setup was modified in the following manner:

The wing was wrapped with a thin layer of sticker. The sticker provided extra strength and durability needed for performing the experiments. The reason for the wing



**FIGURE 26: MODIFIED MODEL WING**

not being able to withstand the boundary conditions is that the epoxy glue alone couldn't keep the whole structure together. The sticker compensated this and provided

the extra support needed to keep the structure together. This ultimately led to producing better and precise results compared to the previous setup.

**Mounting:** The initial mounting of the model wing produced some vibration which added to the free vibration of the model wing and interfered with the output natural frequency. This was caused due to the metal clamps not having any damping.



**FIGURE 27: MOUNTINGS**

To get rid of the metal clamp's vibration an additional metal strip was introduced which connected the two metal clamps together while also fixing the model wing as a cantilever beam. This new mounting reduced the vibration of the metal clamps considerably and produced better results compared to the previous setup.

## 5.9 Final Setup

All the data that were taken for comparison with the simulation values was from the experiments performed on the final setup. Compared to the previous setup, the new modified and redesigned setup produced better results, the experimental values were



FIGURE 28: FULL EXPERIMENTAL SETUP

more precise than before with negligible deflection. The final setup consisted of the following:

- Two metal clamps and a metal strip for mounting the model wing
- Probe hanger for isolating the probe of the EDDY Current Displacement Sensor from the metal clamps for isolating any interference
- Two metal clamps for housing the probe hanger

All the modifications were done for increasing the validity and acceptability of the experimental data.

## 5.10 Experimental Results



FIGURE 29: EXPERIMENTAL RESULT

There were some unavoidable noises which caused fluctuations in the result output. So, for better accuracy the experiment was performed several times. The 1<sup>st</sup> natural frequencies were found to be-

- 24.26 Hz
- 23.82 Hz
- 23.50 Hz
- 23.68 Hz
- 22.85 Hz

From those, we calculated the mean natural frequency to be 23.61 Hz.

## 6 Mode shapes Using Balsa Wood

---

For validating the experimental results with the numerical outputs, we conducted another modal analysis using the material Balsa Wood with similar dimensions, mesh and boundary conditions.

Here the mode shapes and natural frequencies were found to be-

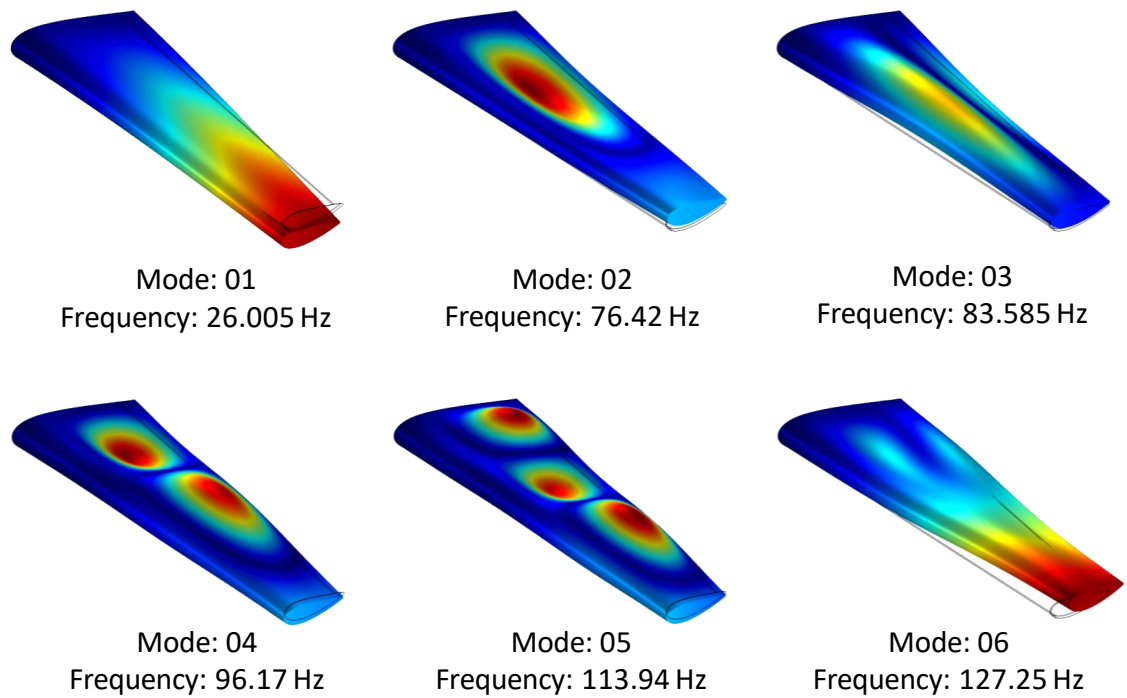


FIGURE 30: MODE SHAPES OF BALSAL WOOD

## 7 Results Comparison

---

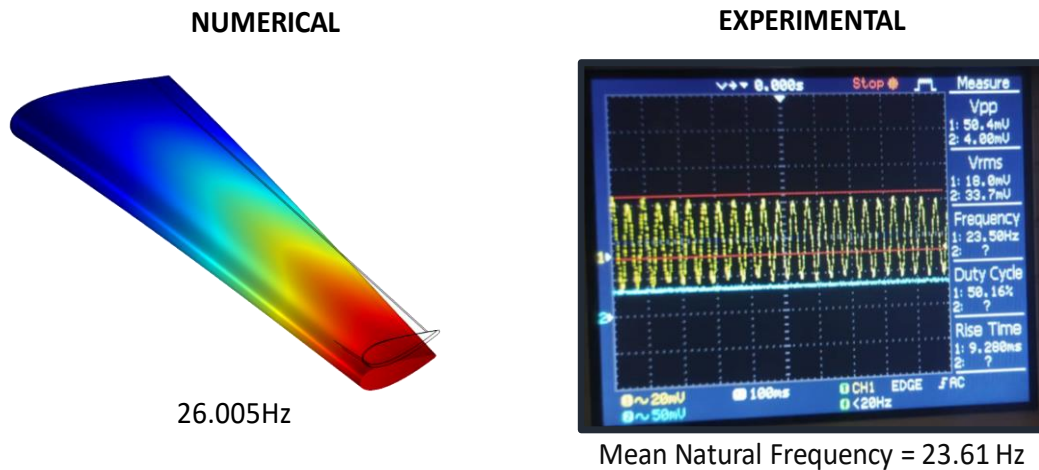


FIGURE 31: RESULT COMPARISON

$$Error = \frac{26.005 - 23.61}{26.005} \times 100\% = 9.20\%$$

## 8 Validation

---

The Computer Aided Design Tools and NACA standards have been accomplished to design the wing structure. The vibration characteristics of the wing structures are studied by modal analysis as well as experimental setup to find the natural frequency of the wing structures. From the above results we can conclude that the difference between the values of natural frequency between the modal analysis and experimental setup are not significant which validates our research work.

## 9 Variations of Design & Model

---

Later on, various modes of vibration along with the respective natural frequencies and mode shapes for hollow, with ribs and solid designs of NACA 4424, NACA 2410, NACA 4412, NACA 16-015 and NACA 633-015 profiles are generated and compared using the same numerical methodology.



## 9.1 NACA 4424

### Numerical Results:

TABLE 5: NATURAL FREQUENCIES (HZ)

Mode	Solid	Without Ribs	With Ribs
1	90.498	97.382	97.497
2	343.97	180.99	313.31
3	353.95	249.14	330.96
4	630.81	258.02	370.78
5	830.63	333.14	417.89
6	1158.1	336.07	508.12
7	1263.2	370.63	539.76
8	1480.3	405.39	572.13
9	1714.5	440.04	625.97
10	1974.7	472.58	654.23

### Result Comparison:

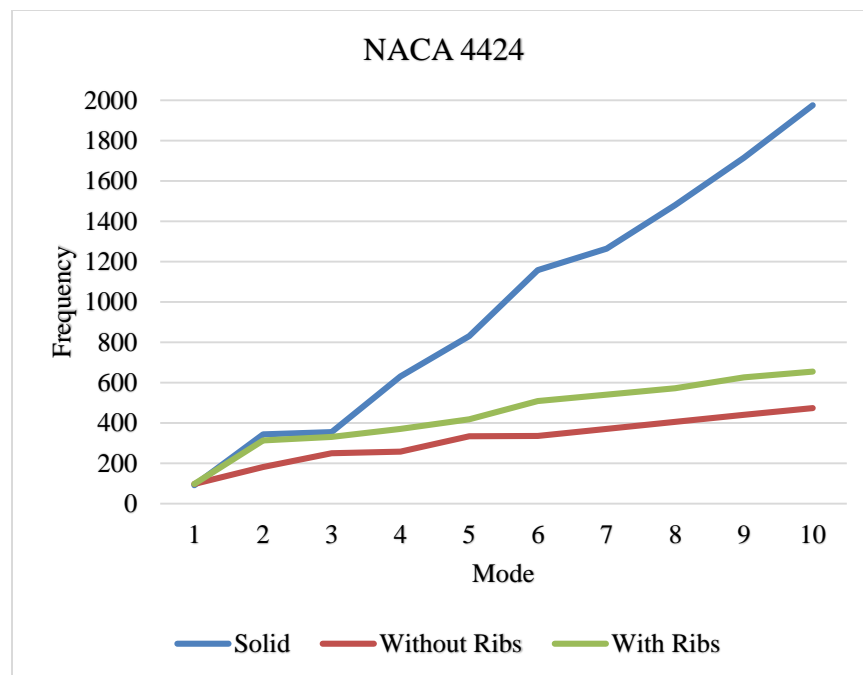


FIGURE 32: FREQUENCY VS MODE GRAPH

## 9.2 NACA 4412

### **Airfoil Profile:**



FIGURE 33: NACA 4412 AIRFOIL PROFILE

### **3D Model:**

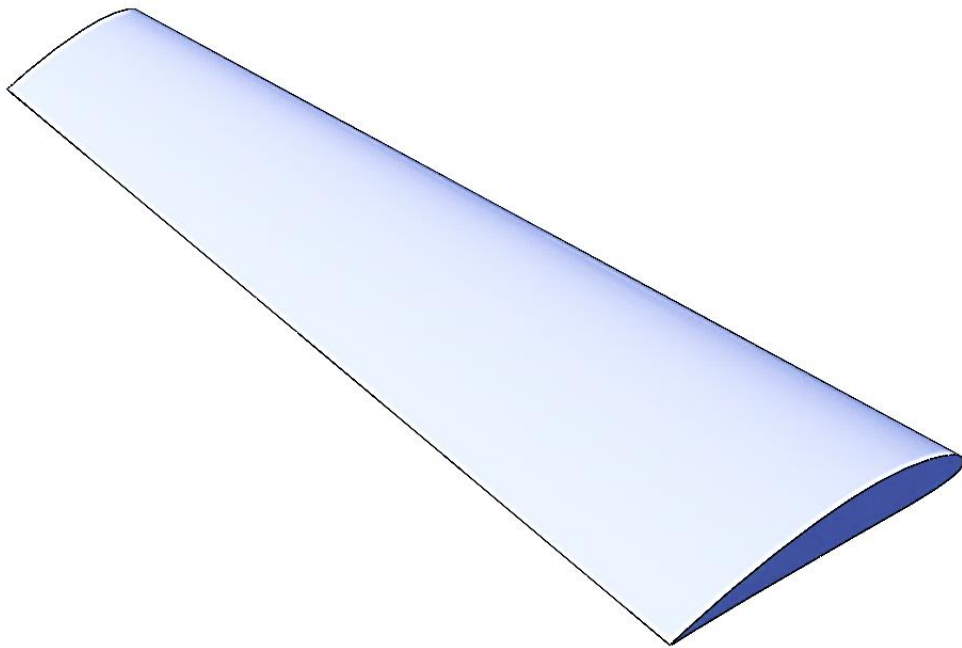


FIGURE 34: NACA 4412 3D MODEL

## Numerical Results:

**TABLE 6: NATURAL FREQUENCIES (Hz)**

Mode	Solid	Without Rib	With Ribs
1	47.146	57.591	57.692
2	185.31	131.2	199.56
3	329.44	181.28	298.28
4	350.75	204.95	314.49
5	440.71	244.06	324.9
6	670.57	283.22	342.69
7	795	311.02	416.54
8	1061	311.33	450.24
9	1165.3	338.43	475.19
10	1212.6	374.87	518.25

## Results Comparison:

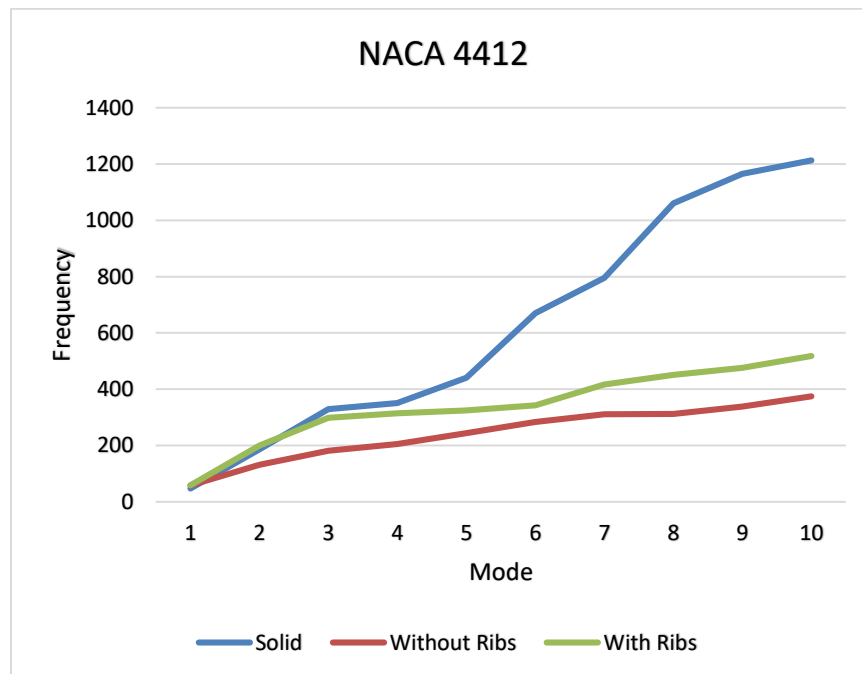


**FIGURE 35: FREQUENCY VS MODE GRAPH**

## 9.3 NACA 2410

### **Airfoil Profile:**

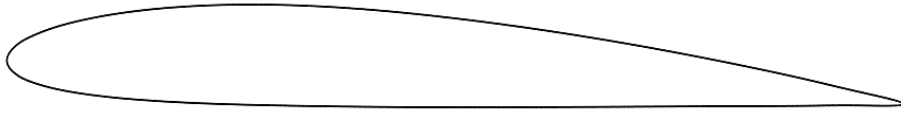


FIGURE 36: NACA 2410 AIRFOIL PROFILE

### **3D Model:**

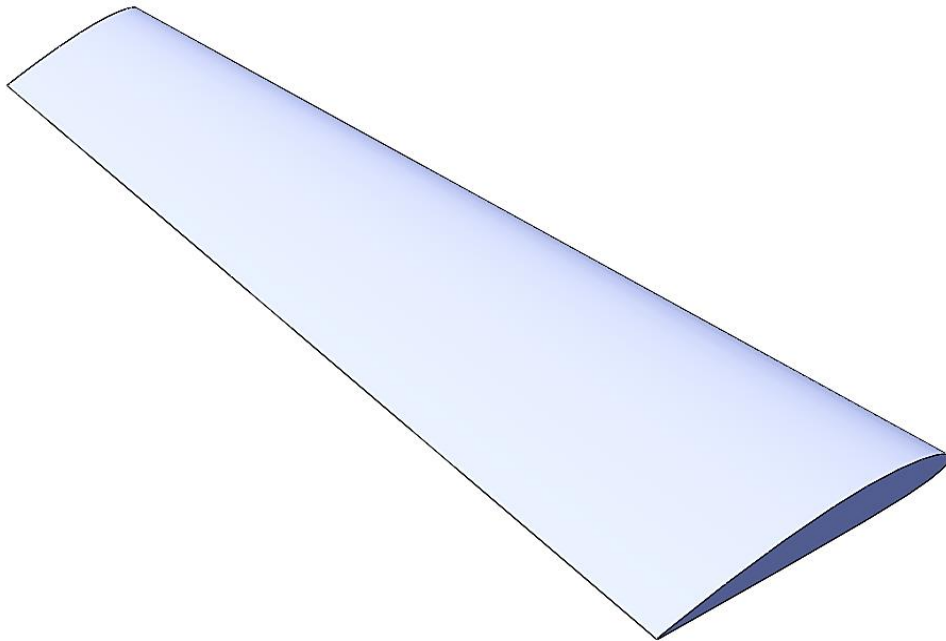


FIGURE 37: NACA 2410 3D MODEL

## Numerical Results:

**TABLE 7: NATURAL FREQUENCIES (Hz)**

Mode No	Solid	Without Ribs	With Ribs
1	38.228	43.018	43.124
2	150.94	150.14	134.92
3	281.41	266.83	195.17
4	344.69	286.36	228.07
5	360.85	332.86	258.14
6	565.44	342.1	268.72
7	655.16	413.55	321.09
8	895.63	452.12	343.91
9	1006	474.33	348.8
10	1162	479.71	385.13

## Results Comparison:

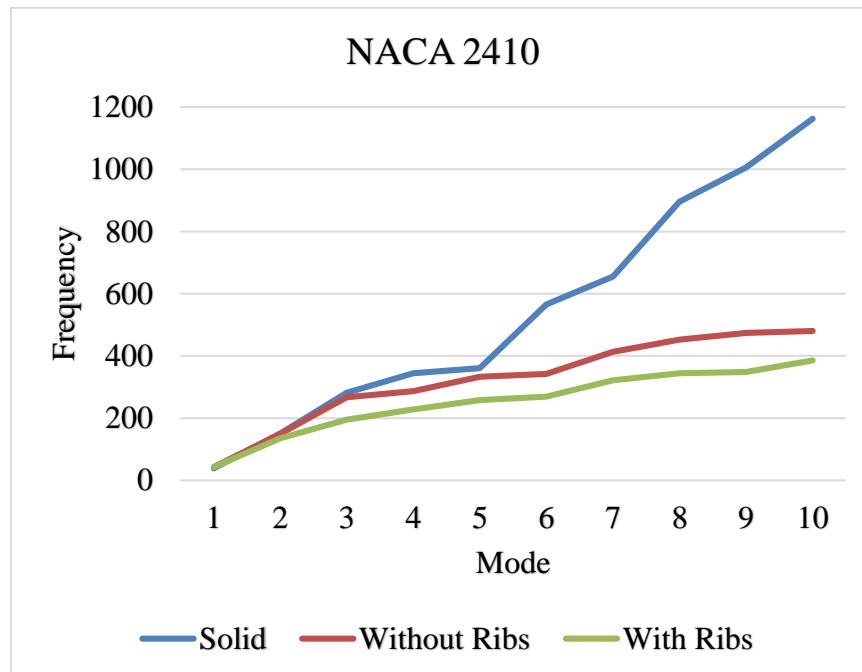


**FIGURE 38: FREQUENCY VS MODE GRAPH**

## 9.4 NACA 16-015

### **Airfoil Profile:**

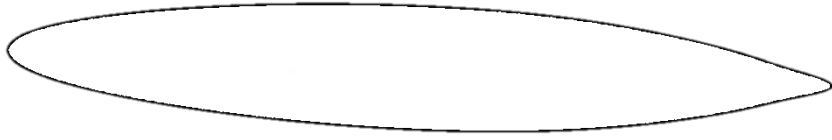


**FIGURE 39: NACA 16-015 AIRFOIL PROFILE**

### **3D Model:**

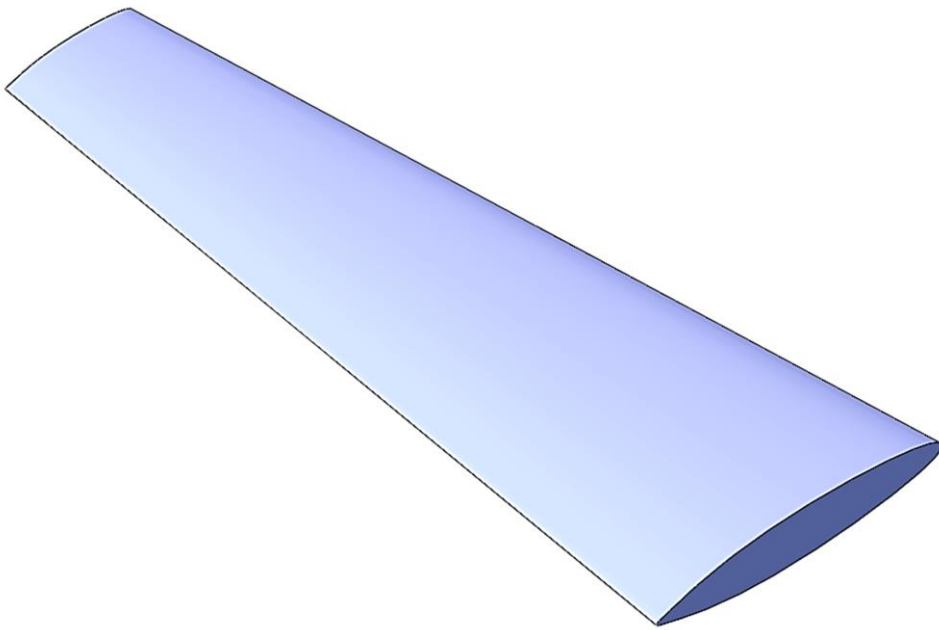


**FIGURE 40: NACA 16-015 3D MODEL**

## Numerical Results:

**TABLE 8: NATURAL FREQUENCIES (Hz)**

Mode	Solid	Without Rib	With Ribs
1	57.5	68.456	67.663
2	227.41	230.29	237.26
3	350.13	232.95	352.34
4	419.54	246.55	380.6
5	546.14	327.57	471.83
6	845.9	345.25	583.13
7	1004.3	356.83	597.82
8	1177.3	445.86	614.23
9	1346.5	451.16	626.69
10	1587.8	479.15	639.64

## Result Comparison:

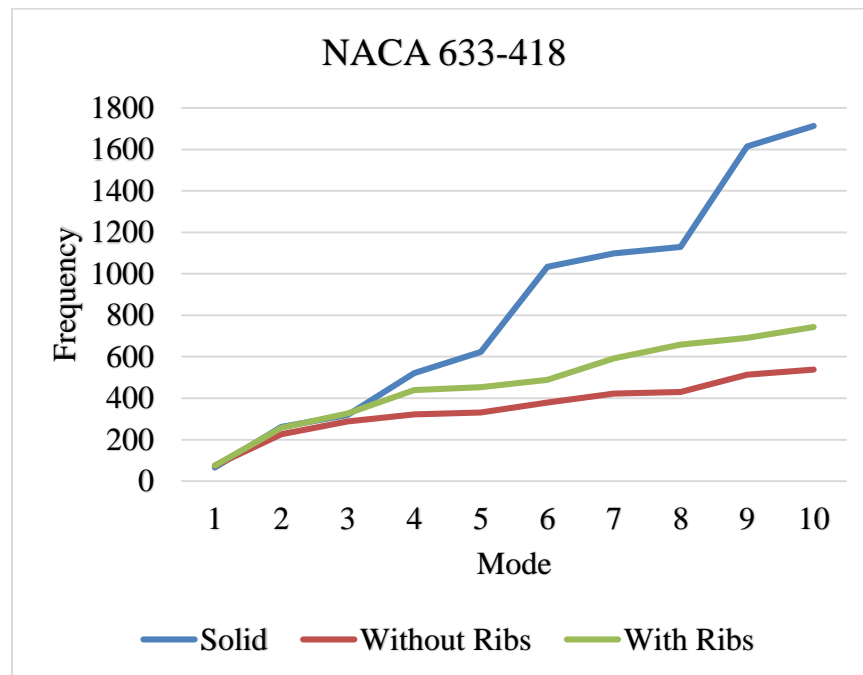


**FIGURE 41: FREQUENCY VS MODE GRAPH**

## 9.5 NACA 633-418

### **Airfoil Profile:**

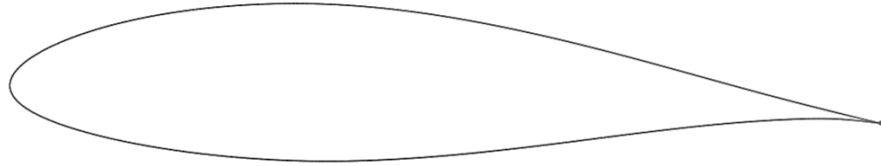


FIGURE 42: NACA 633-418 AIRFOIL PROFILE

### **3D Model:**

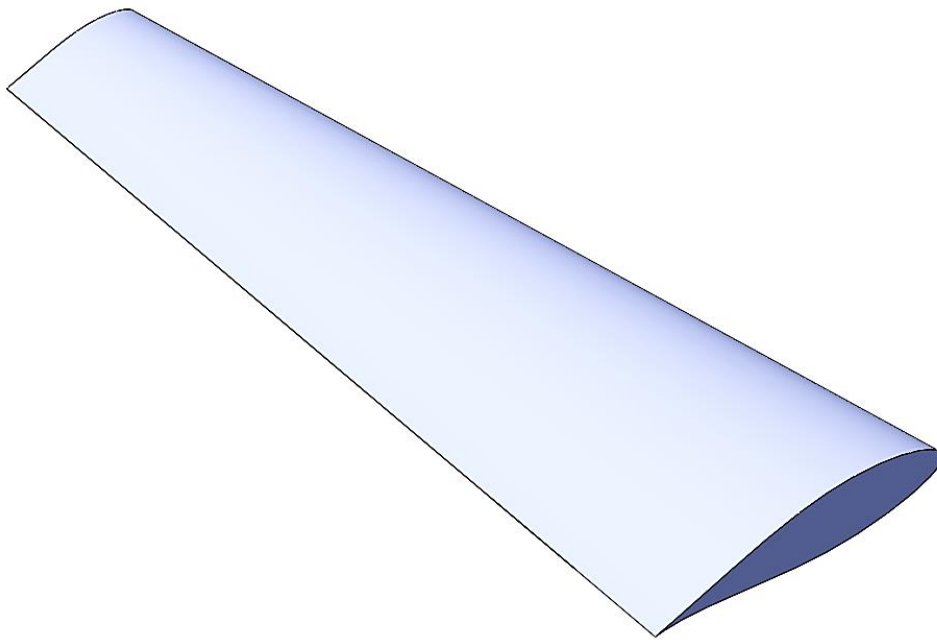


FIGURE 43: NACA 633-418 3D MODEL



## Numerical Results:

TABLE 9: NATURAL FREQUENCIES (Hz)

Mode No	Solid	Without Ribs	With Ribs
1	66.412	75.463	74.875
2	261.44	225.81	257.89
3	318.3	287.63	327.1
4	520.52	321.75	438.87
5	623.02	331.77	453.98
6	1033.8	378.82	488.27
7	1099.2	422.46	592.96
8	1129.7	429.65	658.3
9	1613.9	513.47	690.86
10	1712.4	537.74	743.36

## Result Comparison:

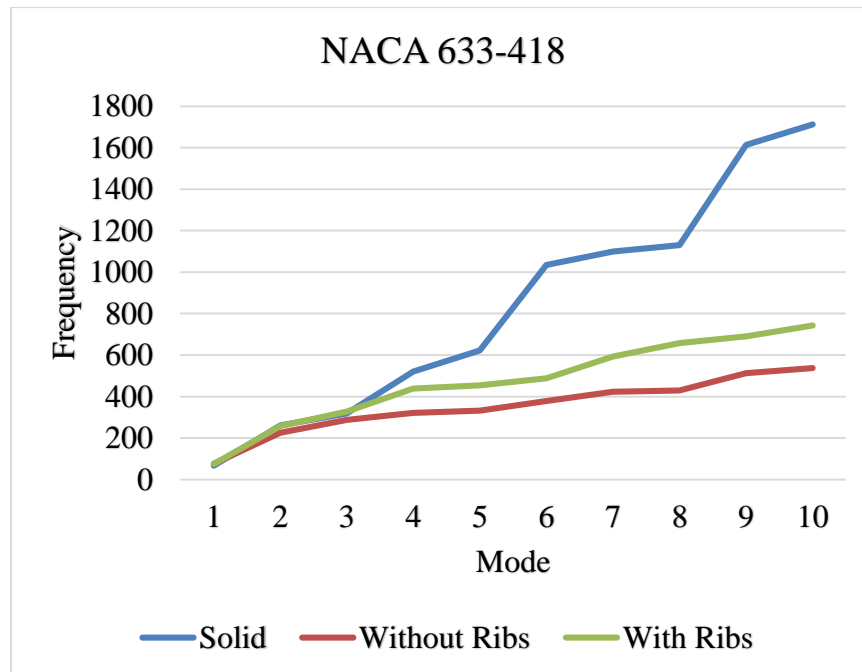


FIGURE 44: FREQUENCY VS MODE GRAPH

## 10 Conclusions

---

The Computer Aided Design Tools and NACA standards have been accomplished to design the wing structure. The vibration characteristics of the wing structures are studied by modal analysis as well as experimental setup to find the natural frequency of the wing structures. From the above results we can conclude that the difference between the values of natural frequency between the modal analysis and experimental setup are not significant. Later we also worked with different NACA profiles with design variation for example solid, slot less & slotted wing. We get the change in frequency response with both design & profile variations. The particular wing design depends upon many factors. Depending on the size, weight, use of the aircraft & desired rate of climb wing design & profile varies. The vibration of the wing is very important factor which affects the aircraft performance. Solid aircraft wing adds a lot of weight on the aircraft results more fuel consumption. Also, in the solid wing the rate of increase of the natural frequency in the mode shapes is larger than any other design which results the increase in the aircraft wing vibration. Slot less wing results low stability to the aircraft. That's why it is not compatible for aircraft wing design. Slotted wing is preferable for aircraft wing design from all perspectives. The vibration of the aircraft wing can be optimized by changing the number of slots. For both numerical & experimental state we considered the aircraft wing as cantilevered beam where one end is fixed & the other end is free. Flutter frequency is the term which is related to when any structure is positioned as cantilevered beam. Flutter is an unstable oscillation which can lead to destruction. Flutter can occur on fixed surfaces, such as the wing or the stabilizer, as well as on control surfaces such as the aileron or the elevator for instance. The natural frequency of the wing adds to the vibration caused by air which causes the risk of reaching flutter frequency. The slots in the airfoil design reduces the vibration and helps the active dampening system of the airplane in avoiding reaching the flutter frequency. During wing vibrations, all motion parameters oscillate, which results in unfavorable working conditions for many onboard systems, for instance the autopilot system. The vibrations badly influence the working environment for crew and travel comfort as well. Wing vibrations have also significant effect on the airframe loading and durability. Varying loads lead to premature tear and wear of wing joints

in the fuselage, suspended devices and mountings of the control surfaces in the wing. Deflections of the wing along the airplane normal axis can produce additional forces acting on ailerons, which may result in bigger wing deflections and loads in the lateral control system.

## 11 Future Scopes

---

For future scopes, the same methodology can be used to compare between various available designs of airfoils like, Low Pitching Moment and High Pitching Moment Airfoils or Flat-bottomed and Symmetrical Airfoils etc. The ideal airfoil design depending on aircraft speed can also be calculated by conducting harmonic analysis for different air pressure.

Wind tunnel test can be conducted both experimentally and numerically for various airfoil profiles and designs. From this test, the natural frequency, total deformation, shear stress, principle stress, total stress for the experimental model wing can be calculated. Using the same methodology, more simulations can be run to figure out these results for both the model airfoil profile and the actual airfoil profiles. This will also open doors for 'Wind Turbine Blades Design' analysis and modification as similar airfoils are used in Wind Turbines.

## 12 References

---

- [1] <http://www.aerospaceweb.org/question/dynamics/q0055.shtml>
- [2] Kakumani Sureka and R Satya Meher,(2015) "Modeling And Structural Analysis On A300 Flight Wing By Using Ansys.", Int. J. Mech. Eng. & Rob. Res. 2015
- [3] K. Sruthi, T. Lakshmana Kishore, M. Komaleswara Rao,(2017),"Design And Structural Analysis Of An Aircraft Wing By Using Aluminum Silicon Carbide Composite."
- [4] Avnish Kumar, "Investigation of Airfoil Design."
- [5] Aswani Kodali and T.N.Charyulu, "Modeling And Analysis On Wing Of A380 Flight"

- [6] Anderson, Jr., J. D., "Aircraft Performance and Design", McGrawHill, 1999
- [7] Dr. R. Rajappan, & V. Pugazhenthii, "Finite Element Analysis of Aircraft Wing Using Composite Structure.", The International Journal of Engineering And Science (IJES) ||Volume|| 2 ||Issue|| 2 ||Pages|| 74-80 ||2013||
- [8] Nikhil A. Khadse & Prof. S. R. Zaweri, "Modal Analysis of Aircraft Wing Using Ansys Workbench.", International Journal of Engineering Resesarch & Technology (IJERT).
- [9] Gultop T., "An Investigation of the effect of aspect ratio on Airfoil performance." Gazi :American Journal of Applied Sciences ISSN/EISSN: 15469239 15543641, Volume: 2, Issue: 2 ,Pages: 545-549 ,1995.
- [10] Lica Flore and Albert Arnau Cubillo " Dynamic Mechanical Analysis of an Aircraft Wing with emphasis on vibration modes change with loading" International Conference of Scientific Paper AFASES 2015 Brasov, 28- 30 May 2015
- [11] Eng. bogdancaloian, Eng. Dorinlozici and eng. Radubisca, 2009 "Stress and Modal Analysis Report for Avert Program", DOI 10.13111/ 2066-8201.
- [12] Mr. Mayurkymarkejadiya, 2013 "CFD Analysis of Pressure Coefficient for NACA 4412"
- [13] <http://www.pdas.com/sections6.html>
- [14] <https://www.aircraftcompare.com/types-of-aircraft-wings/>
- [15] <http://www.lionprecision.com/eddy-current-sensors/ecl202.html#specs>
- [16] <https://www.micro-epsilon.com/displacement-position-sensors/eddy-current-sensor/?sLang=en>
- [17] <https://www.danubewings.com/airfoils-airfoil-terminology-and-definitions>
- [18] [http://www.dave-cushman.net/aircraft/balsa\\_selection.html](http://www.dave-cushman.net/aircraft/balsa_selection.html)

- [19] <https://www.flitetest.com/articles/essencial-rc-airplane-aerodynamics-the-basics>
- [20] <https://images.app.goo.gl/Y6bQBe8sSS11d1tD6>
- [21] <https://images.app.goo.gl/3CK7qH3ZBKuH7YGe6>
- [22] <https://images.app.goo.gl/Vh5byXF649Z9mnWo7>
- [23] <https://images.app.goo.gl/JNPvjcTBWbkF15JL7>
- [24] <https://images.app.goo.gl/4p3c7iWmoceYGxi18>
- [25] <https://images.app.goo.gl/LD9Jdq3ezqcGLHA29>
- [26] <https://images.app.goo.gl/Qsxm8M46Ud9PwbAbA>
- [27] <https://images.app.goo.gl/VV7oruCzLNibYVkv9>
- [28] <https://images.app.goo.gl/1ig4LG5tAX3mk8WU7>
- [29] <https://images.app.goo.gl/3rPHuMyuNuCwnaBSA>
- [30] <https://images.app.goo.gl/2CbJFBMBW18fBWtD8>
- [31] <http://asm.matweb.com/search/SpecificMaterial.asp?bassnum=MA2024T3>
- [32] <https://www.makeitfrom.com/material-properties/Balsa>
- [33] <https://images.app.goo.gl/ius7kFopFdgFFXGy9>
- [34] <https://images.app.goo.gl/zS6Ec1bF7fLfA9KJA>
- [35] <http://home.iitk.ac.in/~mohite>
- [36] <https://m-selig.ae.illinois.edu/ads/aircraft.html>
- [37] <https://whatis.techtarget.com/definition/oscilloscope>